Global dynamics of the May-Leonard system

G. Blé[1], V. Castellanos[1], J. Llibre[2] and I. Quilantán[1]

[1]División Académica de Ciencias Básicas, Universidad Juárez Autónoma de Tabasco, Cunduacán Tabasco, México-2012
[2]Departament de Matemátiques, Universitat Autónoma de Barcelona, Barcelona, Catalonia, Spain.

Introduction

This poster correspond to the paper [2], where you can find the details. In 1975 May and Leonard [1] studied the 3–dimensional Lotka–Volterra differential system

$$\begin{aligned}\dot{x} &= x(1-x-ay-bz),\\ \dot{y} &= y(1-bx-y-az),\\ \dot{z} &= z(1-ax-by-z),\end{aligned} \tag{1}$$

in $x \geq 0$, $y \geq 0$, and $z \geq 0$, describing the competition between three species and depending on two parameters $a > 0$ and $b > 0$.

Let $\mathbb{R}_+ = [0, \infty)$. Assume that $a + b > 2$ and either $a < 1$ or $b < 1$. The carrying simplex $\mathbb{S}$ is the boundary in $\mathbb{R}^3_+$ of the basin of repulsion of the origin of the differential system (1). $\mathbb{S}$ is also the boundary in $\mathbb{R}^3_+$ of the basin of repulsion of the infinity. It is an invariant 2–dimensional surface, homeomorphic to the standard unit simplex, whose boundary contained in $\{x = 0\} \cup \{y = 0\} \cup \{z = 0\}$ attracts all positive orbits except the positive equilibrium point; this boundary was called by May and Leonard a special class of attracting periodic limit cycle solution. In fact it it an attractor heteroclinic cycle in modern language of the qualitative theory of differential equations, detected for the first time in a Lotka–Volterra system and becoming the May–Leonard model so celebrated.

Our objective is to study the completely integrable systems inside the May–Leonard model (1), and to describe its global dynamics in the compactification of $\mathbb{R}^3_+$ in function of the parameters a and b.

If $a + b = 2$ and $a \neq 1$ (otherwise the dynamics is very easy) the global dynamics was partially known, and roughly speaking there are invariant topological half–cones by the flow of the system. These half–cones have a vertex at the origin of coordinates and surround the bisectrix $x = y = z$, and foliate the positive octant. The orbits of each half–cone are attracted to a unique periodic orbit of the half–cone, which lives on the plane $x + y + z = 1$.

If $b = a \neq 1$ then we consider two cases. First $0 < a < 1$ then the unique positive equilibrium point attracts all the orbits of the interior of the positive octant. If $a > 1$ then there are three equilibria in the boundary of positive octant, which attract almost all the orbits of the interior of the octant, we describe completely their bassins of attractions.

1. Main Results

The region of biological interest in the May–Leonard model is the first octant of $\mathbb{R}^3$ which its closure in the Poincaré ball is identified with

$$R = \{(x, y, z) \in \mathbb{R}^3 : x^2 + y^2 + z^2 \leq 1,\ x \geq 0,\ y \geq 0\ z \geq 0\}, \tag{2}$$

and we shall describe the dynamics of the May–Leonard model in R.

Theorem 1. *The May–Leonard differential system* (1) *in* R *is completely integrable if either* $a + b = 2$*, or* $b = a$*.*

Theorem 2. The following statements hold for the May–Leonard differential system restricted to R when $a + b = 2$ and $(a, b) \neq (1, 1)$. All the figures quoted in this theorem correspond to the case $0 < a < 1$, for the case $1 < a < 2$ we must reverse the orientation of all the orbits contained at infinity and at the invariant 2-dimensional simplex $p(\{x + y + z = 1\}) \cap R$.

(a) The phase portrait of the Poincaré compactification of system (1) on the boundaries $p(x = 0)$, $p(y = 0)$ and $p(z = 0)$ of R is topologically equivalent to the one described in Fig. 1(a).

(b) The phase portrait of the Poincaré compactification of system (1) on $R^\infty = \partial R \cap \{x^2+y^2+z^2 = 1\}$, is topologically equivalent to the one described in Fig. 1(b). More precisely, the boundary of R^∞ is a heteroclinic cycle formed by three equilibrium points coming from the ones located at the end of the three positive half–axes of coordinates, and three orbits connecting these equilibria each one coming from the orbit at the end of every plane of coordinates; in the interior of R^∞ we have a center (coming from the end of the invariant bisectrix $x = y = z$), its periodic orbits filled completely the interior of the R^∞.

(c) The plain $x+y+z = 1$ is invariant by the flow of system (1). The phase portrait on the 2–dimensional simplex $R \cap p(\{x + y + z = 1\})$ is topologically equivalent to the one described in Fig. 1(c). The boundary of this simplex is a heteroclinic cycle formed by the equilibrium points $p((1, 0, 0))$, $p((0, 1, 0))$ and $p((0, 0, 1))$ located at the vertices of the simplex, and three orbits connecting these equilibria each one on every side of the simplex; in the interior of the simplex we have a center at the equilibrium $p((1/3, 1/3, 1/3))$, its periodic orbits filled completely the interior of the simplex.

(d) The algebraic surfaces $xyx = h(x + y + z)^3$ with $h \in (0, 1/27]$ are invariant by the flow of system (1), and $R \cap p(xyz = h(x+y+z)^3)$ homeomorphic to the half–cone C_h with vertex at the origin of coordinates and ending at infinity in one of the periodic orbits of the center at infinity drawn in Fig. 1(b) if $h \in (0, 1/27)$, and if $h = 1/27$ then it coincides with $p(x = y = z)$. Every half–cone C_h intersect the simplex $R \cap p(\{x + y + z = 1\})$ in one of the periodic orbits contained in the simplex. Moreover the orbits on C_h below the simplex have their α–limit at the equilibrium point $p((0, 0, 0))$ and their ω–limit at the periodic orbit $p(\{x+y+z = 1\}) \cap C_h$. The orbits on C_h upper the simplex have their α–limit in the periodic orbit at the infinity R^∞ located at the end of the cone C_h and their ω–limit in the periodic orbit $p(\{x + y + z = 1\}) \cap C_h$.

See Fig. 1(d). On the invariant line $R \cap p(\{x + y + z = 1\})$ the equilibrium $p(1/3, 1/3, 1/3)$ attracts the two orbits which has at both sides.

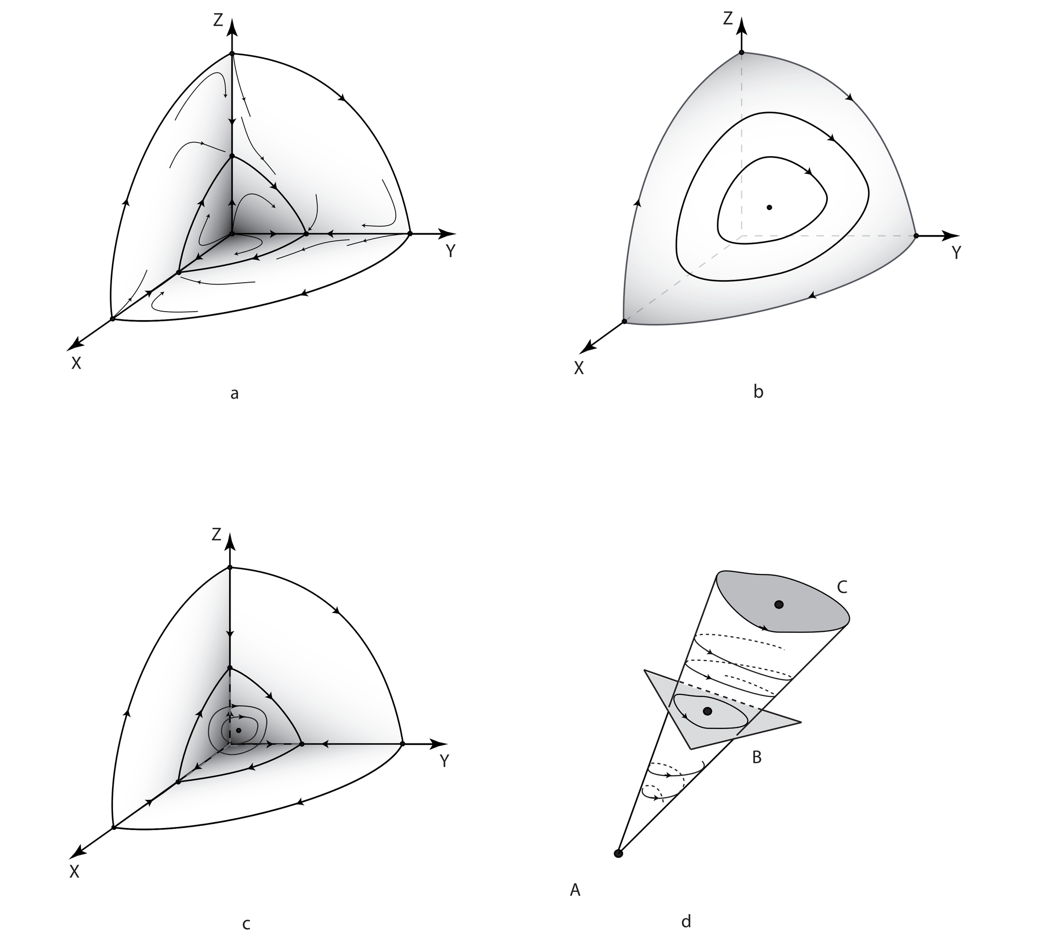

Fig. 1. The global dynamics on the octant R for $a + b = 2$ and $0 < a < 1$.

Proposition 1. The following statements hold for the May–Leonard differential system (1) when $a = b = 1$.

(a) All the straight lines through the origin are invariant.

(b) Let γ be an straight line through the origin of $\mathbb{R}^3$. Then the flow on $p(\gamma) \cap R$ has three equilibria, two at its endpoints. The third equilibrium is on the simplex $R \cap p(\{x + y + z = 1\})$. This last equilibrium attracts the two orbits which has at both sides.

(c) The infinity R^∞ of R and the simplex $R \cap p(\{x + y + z = 1\})$ are filled of equilibria.

Theorem 3. The following statements hold for (1) when $b = a \neq 1$.

(a) The phase portrait of the Poincaré compactification $p(\mathcal{X})$ of system (1) on the boundaries $p(x = 0) \cap R$, $p(y = 0) \cap R$ and $p(z = 0) \cap R$ of R is topologically equivalent to the one described in Fig. 2(a) if $0 < a < 1$ and Fig. 3(a) if $a > 1$.

(b) The plains $x = y$, $y = z$ and $z = x$ are invariant by the flow of system (1), and the phase portrait of $p(X)$ on $p(x = y) \cap R$, $p(y = z) \cap R$ and $p(z = x) \cap R$ are topologically equivalent to the ones described in (b.1), (b.2) and (b.3) of Fig. 2 if $0 < a < 1$ and Fig. 3 if $a > 1$.

(c) The phase portrait of $p(X)$ on R^∞, is topologically equivalent to the one described in Fig. 2(c) if $0 < a < 1$ and Fig. 3(c) if $a > 1$.

(d) The algebraic surfaces $y(x - z) = hx(y - z)$ with $h \in \mathbb{R}$ are invariant by the flow of system (1) and they are elliptic cones for $h \neq 0, 1$. There are three kinds of topological cones $B \cap p(y(x - z) = hx(y - z))$ in the Poincaré ball. First the ones that are restricted to $R \cap p(y(x-z) = hx(y-z))$ contain the image in the Poincaré ball of the half–axes y and z, the negative half–axis x, and the positive part of the bisectrix $x = y = z$. The other two kinds are obtained from the first kind permuting cyclically the letters x, y and z.

The first kind of topological cones $B \cap p(y(x - z) = hx(y - z))$ restricted to R are topological sectors S_h with vertex at the origin $p(0, 0, 0)$, its two sides are the image in the R of the positive half–axes y and z, all the sectors contain the image in R of the positive part of the bisectrix $x = y = z$, and their boundary at infinity. The other two kinds of topological cones also intersect to R in topological sectors which can be described as in the first kind permuting cyclically the letters x, y and z.

The flow on one of these sectors of the first kind S_h is topologically equivalent to the one described in Fig. 2(d) if $0 < a < 1$ and Fig. 3(d) if $a > 1$. Similar figures can be drawn for the sectors of the other two kinds.

(e) If $0 < a < 1$ then all orbits contained in the interior of R have their ω–limit at $P = p(1/(1 + 2a), 1/(1 + 2a), 1/(1 + 2a))$.

Assume $a > 1$. If

$$C = \big(R \cap p(\{x = y \geq z\})\big) \cup \big(R \cap p(\{y = z \geq x\})\big) \cup \big(R \cap p(\{z = x \geq y\})\big),$$

then all the orbits contained in the interior of $R \setminus C$ have their ω–limit in one of the following three attractor equilibria $p(1, 0, 0)$, $p(0, 1, 0)$ and $p(0, 0, 1)$. The three bassins of attraction of these equilibria are separated by the set C.

(f) For $0 < a < 1$ there exists an invariant topological hexagon S of consecutive vertices the equilibria $p(1, 0, 0)$, $p(1/(1 + a), 0, 1/(1 + a))$, $p(0, 0, 1)$, $p(0, 1/(1 + a), 1/(1 + a))$, $p(0, 1, 0)$ and $p(1/(1 + a), 1/(1 + a), 0)$, and sides on $p(x = 0) \cap R$, $p(y = 0) \cap R$ and $p(z = 0) \cap R$. The vertices alternate saddles with repeller nodes being $p(1, 0, 0)$ a repelling node. In the interior of this topological hexagon there is the equilibrium P which is an attracting node. The flow on S is topologically equivalent to the one described in Fig. 2(e).

For $a > 1$ there exists an invariant topological hexagon S with the same vertices and sides on the planes of coordinates. The vertices alternate saddles with attracting nodes being $(1, 0, 0)$ an attracting node. In the interior of this topological hexagon there is the equilibrium p which is a repeller node. The flow on S is topologically equivalent to the one described in Fig. 3(e).

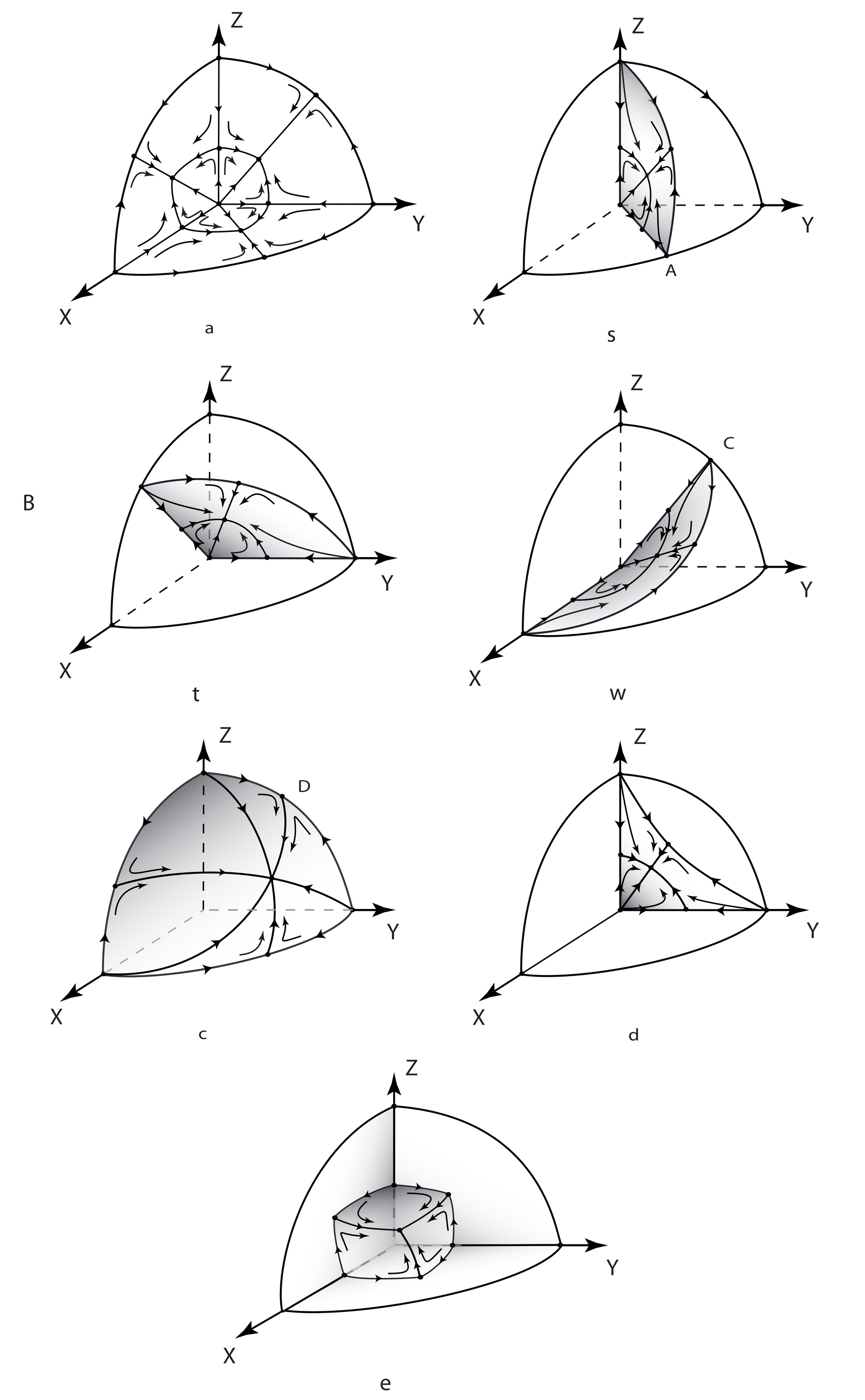

Fig. 2. The global dynamics on the octant R for $b = a < 1$.

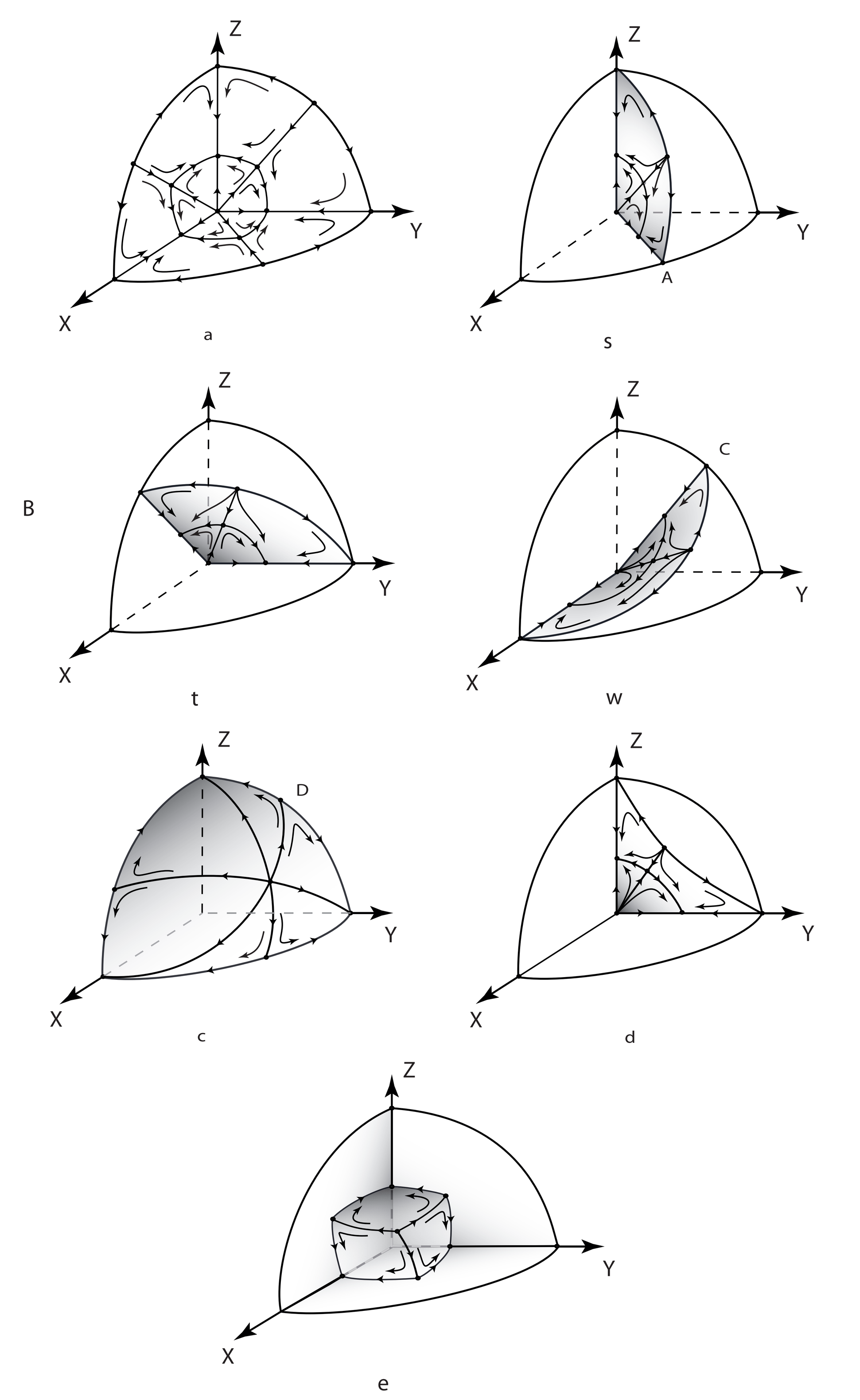

Fig. 3. The global dynamics on the octant R for $b = a > 1$.

References

[1] R. M. May, W. J. Leonard. *Nonlinear aspects of competition between three species.* SIAM J. Appl. Math. 29 (1975), 243 - 253.

[2] G. Blé, V. Castellanos, J. Llibre, I. Quilantán. *Integrability and global dynamics of the May-Leonard model.* Nonlinear Anal. Real World Appl. 14 (2013), 280 - 293.